SCIENTIFIC REPORTS

OPEN

Received: 04 November 2016
Accepted: 09 January 2017
Published: 10 February 2017

Top-down, decoupled control of constitutive parameters in electromagnetic metamaterials with dielectric resonators of internal anisotropy

Sukmo Koo†, Daniel R. Mason, Yunjung Kim & Namkyoo Park

A meta-atom platform providing decoupled tuning for the constitutive wave parameters remains as a challenging problem, since the proposition of Pendry. Here we propose an electromagnetic meta-atom design of internal anisotropy ($\varepsilon_r \neq \varepsilon_\theta$), as a pathway for decoupling of the effective- permittivity ε_{eff} and permeability μ_{eff}. Deriving effective parameters for anisotropic meta-atom from the first principles, and then subsequent inverse-solving the obtained decoupled solution for a target set of ε_{eff} and μ_{eff}, we also achieve an analytic, top-down determination for the internal structure of a meta-atom. To realize the anisotropy from isotropic materials, a particle of spatial permittivity modulation in r or θ direction is proposed. As an application example, a matched zero index dielectric meta-atom is demonstrated, to enable the super-funneling of a 50λ-wide flux through a sub-λ slit; unharnessing the flux collection limit dictated by the λ-zone.

Electromagnetic metamaterials exhibiting naturally non-occurring refractive indices[1–24] and their application to exotic forms of wave manipulation[25–29] have become one of the hottest research topics. Because electromagnetic metamaterials manifest their properties through electromagnetic couplings to the far-field, design strategies have been focused on the realization of designer electric (ε_{eff}) and magnetic (μ_{eff}) dipolar responses, with the engineering and assembly of metallic or dielectric building blocks. Nonetheless, in most cases, the realization of exotic ε_{eff} and μ_{eff} has been achieved via the simple combination of elementary resonators in a non-isotropic and polarization-dependent form[1,2,25], at the same time based on retro-fit, bottom-up approaches - where the building blocks are initially proposed and the subsequent design is carried out through a series of iterations and guesswork.

Meanwhile, although the decoupling of those fundamental constitutive wave parameters has been envisaged as an ideal platform toward the top-down and deterministic design of the metamaterial (Pendry *et al.*[26]), its feasibility has not been treated until recently. With the presence of inherent cross-coupling terms between constitutive parameters (as shown for ε_{eff} and μ_{eff} in electromagnetics[3], or B_{eff}^{-1} and ρ_{eff} in acoustics[30]), it is not always straightforward to achieve the decoupling of wave parameters. Elastic metamaterial for decoupling of density and stiffness in positive[31] or negative[32] parameter regime, sub skin-depth metallic particles of decoupled permittivity and permeability for positive high refractive index[4,5], and lastly the acoustic omni meta-atom[30] addressing the octant space of wave parameters have been demonstrated; yet existence of the meta-atom platforms which could access both positive and negative values of parameters, in the general spectrum of electromagnetic wave is not evident at this stage. Moreover, we note that the design of electromagnetic metamaterial has been largely based on metallic inclusions of well-defined current paths, meanwhile the intrinsic loss of metals makes dielectric metamaterial[1,6–10] a more favorable option.

Photonic Systems Laboratory, Department of Electrical and Computer Engineering, Seoul National University, Seoul 08826, Korea. †Present address: Moore Laboratory, Department of Medical Engineering, California Institute of Technology, Pasadena, California 91125, USA. Correspondence and requests for materials should be addressed to N.P. (email: nkpark@snu.ac.kr)

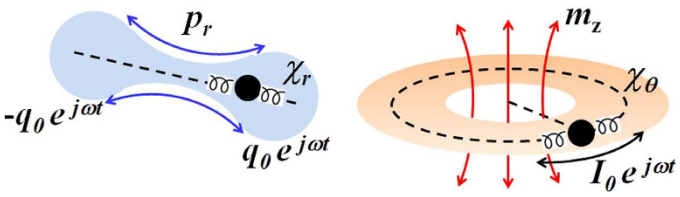

Figure 1. Physical origin of the electron induced electric (left) and magnetic (right) dipole moments of a classical atom.

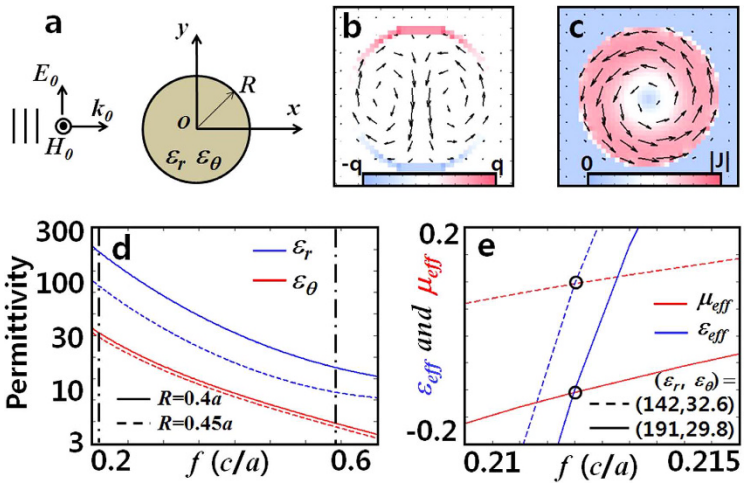

Figure 2. (**a**) Schematic of the anisotropic meta-atom illuminated by TE plane wave. (**b**) Charge and (**c**) current distribution at the electric and magnetic resonance frequencies, respectively (arrows denote current flow). (**d**) Calculated ε_r and ε_θ values that give matched zero index property (solid: $R = 0.4a$, dashed: $R = 0.45a$). (**e**) ε_{eff} and μ_{eff} tunability including demonstration of matched index property ($n_{\text{eff}} = \pm 0.1$).

Here, we propose a new platform for electromagnetic metamaterial: a meta-atom of decoupled constitutive parameters, enabling top-down design - where the target ε_{eff} and μ_{eff} are first specified and the design parameters are subsequently determined, all the while using readily available lossless dielectrics. We first analytically solve the problem of decoupled effective- permittivity ε_{eff} and permeability μ_{eff}, by introducing a hypothetical meta-atom of internal anisotropic susceptibility $\chi_r \neq \chi_\theta$; for their axis are set in conform to the electric- and magnetic- characteristic movements of the electron, or equivalently to their corresponding dipole moments p_r (χ_r) and m_z (χ_θ) (Fig. 1). We then realize top-down design for the internal structure of a meta-atom, by inversely-solving the decoupled equation to get the required χ_r and χ_θ (or ε_r and ε_θ) for targeted ε_{eff} and μ_{eff}. Finally, a meta-atom implementation based on isotropic materials of spatial (r, θ) permittivity modulation is proposed to realize the required (ε_r, ε_θ) for a matched zero index, along with the demonstration of the super-funneling for a 50λ-wide flux through a sub-λ slit.

Results

Structure of the meta-atom for decoupled permittivity and permeability. We consider the two dimensional problem shown in Fig. 2(a); where a transverse electric (TE) plane wave is incident onto a cylindrical particle of radius R with split ε_r, ε_θ anisotropy. To derive ε_{eff} and μ_{eff}, we start from the zeroth order expressions for the electric and magnetic polarizabilities (α_e and α_m)[11] of the isolated particle,

$$\begin{aligned} \alpha_e &= \frac{\int_C (\varepsilon_y - 1) E_y ds}{E_0}, \\ \alpha_m &= -\frac{j\omega}{2H_0} \int_C \varepsilon_0 (\varepsilon_\theta - 1) \mathbf{r} \times \mathbf{E} ds, \end{aligned} \tag{1}$$

where ε_y and ε_θ being the permittivity of the particle along the y and θ direction respectively, and the integration is taken over the particle cross section C. It is noted that in Eq. (1) we treat only the dipole polarizability terms, with an implicit assumption of long-wavelength approximation. Solving the wave equation in polar coordinate for the general solution of **E** and **H** (details in Supplementary Information), and then keeping only the lowest order terms (within good approximation under ε_r, $\varepsilon_\theta \gg 1$), we achieve analytical solutions for α_e and α_m,

$$\begin{aligned} \alpha_e &\sim \pi R c J_{\sqrt{\frac{\varepsilon_\theta}{\varepsilon_r}}}(\sqrt{\varepsilon_\theta}\phi_k) b_1, \\ \alpha_m &\sim j\omega\pi R^2 J_2(\sqrt{\varepsilon_\theta}\phi_k) b_0, \end{aligned} \tag{2}$$

where $\phi_k = k_0 R$ and b_n being the coefficients of Bessel-Fourier expansions [Supplementary Eq. (S3)].

From α_e and α_m of the isolated particle (2), it is then straightforward to calculate ε_{eff} and μ_{eff} for a square lattice of meta-atoms. Using the mixing formula[12] we arrive,

$$\begin{aligned} \varepsilon_{\text{eff}} &= f(\alpha_e, C_{\parallel}), \\ \mu_{\text{eff}} &= f(\alpha_m, C_{zz}), \end{aligned} \tag{3}$$

where $f(\alpha, C) \approx 1 + \frac{1}{a^2}\frac{1}{\text{Re}[\alpha^{-1}] - \text{Re}[C]}$ and $C_{\parallel} \approx \frac{k_0^2}{2}\sum_{\mathbf{r_I}\neq\mathbf{0}} H_0^{(2)}(k_0|\mathbf{r_I}|) + \frac{1}{a^2}$, $C_{zz} \approx 2C_{\parallel} - \frac{1}{a^2}$ are the dynamic interaction constants with periodicity a, and a lattice point vector $\mathbf{r_I}$[12].

Inspection of Eqs (2) and (3) clearly shows the dependence of μ_{eff} only on ε_θ, or complete decoupling of μ_{eff} (or α_m) from ε_r, which supports separate tunability of ε_{eff} and μ_{eff} from the adjustment of ε_r and ε_θ; confirming the proposed ansatzs based on anisotropic susceptibility in relation to the respective current patterns exhibited by the electric and magnetic modes [Figs 1 and 2(b,c)]. Because the obtained decoupling condition $\alpha_e(\varepsilon_r, \varepsilon_\theta)$ and $\alpha_m(\varepsilon_\theta)$ are based on (2) - which are expanded from (1), the condition of decoupling becomes to follow the generic constraint of long-wavelength approximation in metamaterial applications; lattice period (a)/wavelength (λ/n_{eff}) ~ 1/10. For example, with $a = 5\lambda$, the validity of our approximation would hold till $|n_{\text{eff}}| < 0.5$. We also note, Eq. (3) works well in the low index regime ($n_{\text{eff}} \ll \lambda/2a$[12]), while ε_{eff} and μ_{eff} of high values also always can be determined from S-matrix parameters[13].

Focusing here on the low index case, we now proceed to *inverse*-solve the problem of (3), in order to determine required $\varepsilon_r(\alpha_e)$ and $\varepsilon_\theta(\alpha_e, \alpha_m)$ by using (2), from *target* ε_{eff} and μ_{eff}. Meanwhile the complete solution with Bessel-Fourier series (Supplementary Eq. (S3)) can also be used, here we show the simpler form of first-order approximated solution, near the first zeros of the Bessel functions[11] (see Supplementary Information for details). For example, by specifying target ε_{eff} and μ_{eff} equal to 0, we arrive to a set of simple and intuitive relations which are used to calculate the required values of ε_r and ε_θ for the matched zero index;

$$\begin{aligned} \phi_k &\cong \frac{\alpha_0 - A_0(\phi_k)}{\sqrt{\varepsilon_\theta}} + \frac{\alpha_1 - \alpha_0}{\sqrt{\varepsilon_r}}, \\ \phi_k &\cong \frac{\alpha_1}{\sqrt{\varepsilon_\theta}} - B_0(\phi_k), \end{aligned} \tag{4}$$

where $A_0(\phi_k) = A(\varepsilon_{\text{eff}} = 0; \phi_k)$ and $B_0(\phi_k) = B(\mu_{\text{eff}} = 0; \phi_k)$ are slowly-varying functions of ϕ_k (Supplementary Eq. (S6) and Supplementary Fig. S1), and α_0 (~2.405), α_1 (~3.831) are the first zeros of the zeroth and first order Bessel functions. Again, for a given particle radius and frequency $\phi_k = k_0 R$, the achievement of $\mu_{\text{eff}} = 0$ from the *single* parameter ε_θ is evident from $B(\mu_{\text{eff}} = 0; \phi_k)$ in Eq. (4). Subsequent realization of $\varepsilon_{\text{eff}} = 0$ from the determination of ε_r is made then using $A(\varepsilon_{\text{eff}} = 0; \phi_k)$ in (4). In Fig. 2(d) we show the solution obtained with Supplementary Eq. (S5), giving the values of $(\varepsilon_r, \varepsilon_\theta)$ that support a matched zero index at different target frequencies; for the particles of normalized radius $R = 0.4a$ (solid lines) and $0.45a$ (dashed lines), of periodicity (a). The required $(\varepsilon_r, \varepsilon_\theta)$ value set depends on the frequency and particle size, and get smaller as either f or R increase. We also demonstrate in Fig. 2(e) the tunability of ε_{eff} and μ_{eff} by addressing matched index properties at $n_{\text{eff}} = \pm 0.1$, again, with the use of (3). It is worth to note that in all cases, the required ε_r is greater than ε_θ, red-shifting the usually higher energy electric dipole resonance $(\varepsilon_r, \varepsilon_\theta)$ closer toward the lower energy magnetic dipole resonance (ε_θ).

Dielectric implementation of the anisotropic meta-atom. To realize the set of required ε_r and ε_θ from isotropic materials, we spatially modulate the permittivity inside the particle along a given axis ($\mathbf{r}$ or $\boldsymbol{\theta}$). A proposed structure of nano-pizza cross-section is shown in Fig. 3(a). Extending the concept of average permittivity[33] from Gauss' law in polar coordinates we obtain,

$$\varepsilon_r \sim (1-p)\varepsilon_1 + p\varepsilon_2, \quad \varepsilon_\theta \sim \left(\frac{1-p}{\varepsilon_1} + \frac{p}{\varepsilon_2}\right)^{-1}, \tag{5}$$

where $\varepsilon_1, \varepsilon_2$ $(\varepsilon_1 < \varepsilon_2)$ are the permittivities of constituent dielectrics shown in Fig. 3(a), and p is the fill factor of slices containing ε_2. While it is also possible to design the meta-atom for fixed ε_1 (1, for example) by changing p and ε_2, we here focus on the case of fill factor $p = 0.5$, without any loss of generality (design example with $p = 0.83$, for $\varepsilon_1 = 1$ (air) and $\varepsilon_2 = 12.25$ (silicon) is shown in the Supplementary Information). On the other hand, as the arithmetic mean is always larger than the harmonic mean in (5), the condition of $\varepsilon_r \geq \varepsilon_\theta$ for matched zero index realization [Fig. 2(d)] is only met with nano-pizza cross-section geometry [we note, $\varepsilon_\theta \geq \varepsilon_r$ for the nano-donut cross-section - inset of Fig. 3(a)]. Using (5) for the pair $(\varepsilon_r, \varepsilon_\theta) = (166, 31.1)$ [giving zero index at $f = 0.212\ c/a$ (4.24 GHz for $a = 1.5$ cm) and $R = 0.4a$ from Fig. 2(d)], we obtain $(\varepsilon_1, \varepsilon_2) = (16.32, 315.8)$.

In Fig. 3(c) we show plots of $\varepsilon_{\text{eff}}(\alpha_e)$ and $\mu_{\text{eff}}(\alpha_m)$ obtained from Eq. (3), with α_e and α_m analytically obtained from Eq. (2) (solid lines), and also numerically obtained using Eq. (1) (solid dots) from the result of finite difference time domain simulations of a 40-slice structure. Near the zero-index, an almost perfect fit with less than 1% frequency error was obtained from that predicted by Supplementary Eq. (S5). In consideration of fabrication

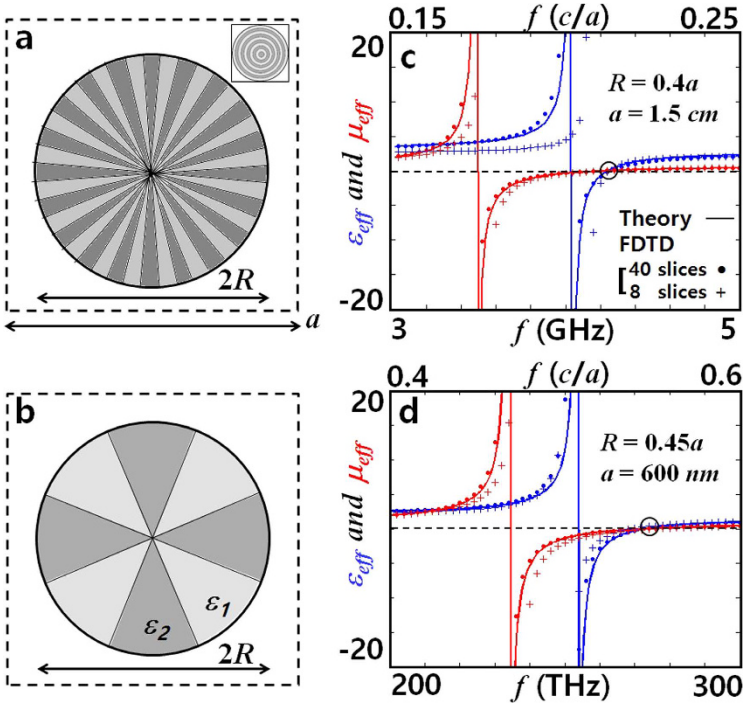

Figure 3. Anisotropic meta-atoms ($\varepsilon_r \neq \varepsilon_\theta$) of nano-pizza cut geometry with (**a**) 40 slices and (**b**) 8 slices. (inset in (a) shows an example of nano-donut). Calculated ε_{eff} and μ_{eff} for meta-atoms lattice of radius (**c**) $R = 0.4a$ ($a = 1.5$ cm), and (**d**) $R = 0.45a$ ($a = 600$ nm). By appropriate choice of a, the operating frequency is determined. Circles indicate the frequencies of operation at matched zero index and horizontal dashed lines indicate $\varepsilon_{\text{eff}} = 0$ and $\mu_{\text{eff}} = 0$. Excellent agreement between the theory and numerical results (for both 40 slice and 8 slice implementations), especially near the matched zero index, are observed.

complexity, a structure with reduced number of slices has also been tested [Fig. 3(b)]. Even though the calculation of (ε_r, ε_θ) from (p; ε_1, ε_2) started to deviate from Eq. (5) when the size of slices was increased, it was still possible to determine (ε_1, ε_2) = (15.12, 171.9) providing a matched zero index for the 8-slice structure at $f = 0.212$ c/a [marked with '+' symbol in Fig. 3(c)], by using few Newton iterations for the zero-index frequency deviation. It is noted that this value determined from the mixing formula (3) is in excellent agreement with exact values of (ε_1, ε_2) = (14.53, 179.2) extracted from S-matrix parameters[13].

It is emphasized that, experimentally available, smaller permittivity values using Si and SiO_2 for example [40 slices: (ε_1, ε_2) = (2.43, 15.13), 8 slices: (2.22, 12.96)], can be readily accessed by increasing the radius R of the particle to $0.45a$, to give matched zero index at $f = 0.546$ c/a (e. g., $\lambda = 1100$ nm for $a = 600$ nm) [Fig. 3(d)]. The designs with 2D-slab structure (of height $= 2\lambda$, at GHz operation frequency) and a void at the particle center region are also discussed in Supplementary Information and Figures.

Realization of the zero index super funneling through a subwavelength slit. Using the matched zero index, we now investigate the problem of extraordinary optical transmission (EOT)[34–38], for which the maximum field enhancement is limited by the λ-zone[34]. Applications of zero index tunneling have been demonstrated in the past[11,14–16], yet the possibility of EOT beyond the λ-zone has not been investigated. A perfect electric conductor (PEC) having sub-wavelength (0.21λ) slit, of flux reception width far larger (17λ) than the λ-zone has been tested, with the application of single-layer matched zero index meta-atoms ($\varepsilon_{\text{eff}} = \mu_{\text{eff}} = 0$, $f = 0.212$ c/a) covering the input/output regions of PEC. It is important to note that the tuning of meta-atom near the slit gap is necessary since the effective medium theory starts to deviates with the introduction of the metal slit in the meta-atom array, breaking the periodicity of the lattice. The detailed tuning procedure is described in the Supplementary Information. The transmittance of the matched zero-index meta-atom nanoslit shows almost perfect transmittance of 0.97 [Fig. 4(a,d)], a ~50 times increase compared to the slit without zero-index meta-atom coating [Fig. 4(a,e)]; demonstrating the super-funneling of flux which is 17 times greater than the λ-zone. A low-index 8-slice structure [(ε_1, ε_2) = (2.22, 12.96) at $R = 0.45a$ providing matched zero index at $f = 0.546$ c/a, see Fig. 3(d)] over much larger flux reception area (50λ) also has been tested, to compensate for a factor of ~90 channel width variation (50λ to 0.55λ). A transmittance of 0.85 was achieved, showing the super-funneling of 42λ-flux ($50\lambda \cdot 0.85$) through the meta-atom coated slit [Fig. 4(a,f)].

Discussion

To summarize, a hypothetical meta-atom of internal (r, θ) anisotropy has been proposed. Introducing the split-symmetry of susceptibility $\chi_r \neq \chi_\theta$ conforming to the orthogonal axes of current pathways of the respective

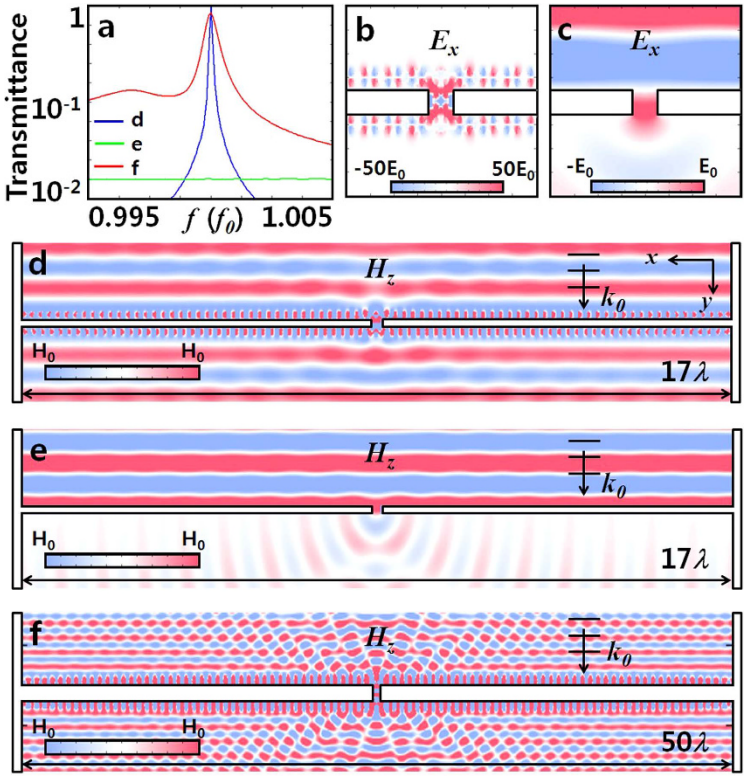

Figure 4. (**a**) Transmission spectra of the slit; without (green) and with matched zero-index meta-atom array of (blue) high index (ε_1, ε_2) = (14.53, 179.2) and (red) low index (2.22, 12.96) materials. f_0 is the frequency of matched zero index. (**b**,**c**) E_x field pattern near the nanoslit at f_0; (**b**) with and (**c**) without the zero-index meta-atom array. The near field pattern shows the associated dramatic enhancement of the electric field with the coating of matched zero index meta-atoms. (**d**–**f**) H_z field pattern of the slit at f_0 (**d**) without, (**e**) with high-index, and (**f**) with low-index meta-atom array. Slit width; 0.21λ (**d**,**e**) and 0.55λ (**f**).

electric- and magnetic- dipoles, we show analytically the decoupling and separate tunability of ε_{eff} and μ_{eff}. The desired target optical response ε_{eff} and μ_{eff} are provided by top-down, analytically determined ε_r and ε_θ values, which are readily achieved with conventional isotropic materials in radial- or angular- anisotropic spatial arrangements. We note that, our approach widens the scope of metamaterial design; offering a top-down optical response (including both matched zero and negative index) from lossless dielectrics, meanwhile lifting the stringent restrictions of accidental degeneracy[6] which itself was limited to matched zero index at fixed frequency. In an application to EOT, utilizing a single layer of matched zero index meta-atoms, we demonstrated for the first time a super-funneling of electromagnetic flux, overcoming the usual λ-zone limit by two orders. Our proposal of coordinate-conforming anisotropy for decoupling the electric and magnetic responses and thus the separate control of ε_{eff} and μ_{eff} should be applicable to elementary resonators in other exotic coordinate systems compliant to current pathways of chosen electric/magnetic resonances. We expect future development of other anisotropic meta-atom families based on our approach.

References

1. Ahmadi, A. & Mosallaei, H. Physical configuration and performance modeling of all-dielectric metamaterials. *Phys. Rev. B* **77,** 045104 (2008).
2. Zhang, S. *et al.* Near-infrared double negative metamaterials. *Opt. Express* **13,** 4922–4930 (2005).
3. Alù, A. First-principles homogenization theory for periodic metamaterials. *Phys. Rev. B* **84,** 075153 (2011).
4. Kim, J. Y. *et al.* Highly tunable refractive index visible-light metasurface from block copolymer self-assembly. *Nat. Commun.* **7,** 12911 (2016).
5. Chung, K., Kim, R., Chang, T. & Shin, J. Optical effective media with independent control of permittivity and permeability based on conductive particles. *Appl. Phys. Lett.* **109,** 021114 (2016).
6. Huang, X., Lia, Y., Hang, Z. H., Zheng H. & Chan, C. T. Dirac cones induced by accidental degeneracy in photonic crystals and zero-refractive-index materials. *Nat. Materials* **10,** 582–586 (2011).
7. Li, Y. *et al.* On-chip zero-index metamaterials. *Nat. Photon.* **9,** 738–742 (2015).
8. Zhao, Q., Zhou, J., Zhang, F. & Lippens, D. Mie resonance-based dielectric metamaterials. *Mater. Today* **12,** 60–69 (2009).
9. Soukoulis, C. M. & Wegener, M. Past achievements and future challenges in the development of three-dimensional photonic metamaterials. *Nat. Photonics* **5,** 523–530 (2011).
10. Vendik, I. B., Vendik, O. G. & Gashinova, M. S. Artificial dielectric medium possessing simultaneously negative permittivity and magnetic permeability. *Tech. Phys. Lett.* **32,** 429–433 (2006).
11. Silveirinha, M. & Engheta, N. Design of matched zero-index metamaterials using nonmagnetic inclusions in epsilon-near-zero media. *Phys. Rev. B* **75,** 075119 (2007).

12. Silveirinha, M. G. Nonlocal homogenization model for a periodic array of ε-negative rods. *Phys. Rev. E* **73,** 046612 (2006).
13. Smith, D. R., Schultz, S., Markoš, P. & Soukoulis, C. M. Determination of effective permittivity and permeability of metamaterials from reflection and transmission coefficients. *Phys. Rev. B* **65,** 195104 (2002).
14. Edwards, B., Alů, A., Young, M. E., Silveirinha, M.& Engheta, N. Experimental Verification of Epsilon-Near-Zero Metamaterial Coupling and Energy Squeezing Using a Microwave Waveguide. *Phys. Rev. Lett.* **100,** 033903 (2008).
15. Cheng, Q., Liu, R., Huang, D., Cui, T. J. & Smith, D. R. Circuit verification of tunneling effect in zero permittivity medium. *Appl. Phys. Lett.* **91,** 234105 (2007).
16. Silveirinha, M. & Engheta, N. Tunneling of electromagnetic energy through subwavelength channels and bends using ε-near-zero materials. *Phys. Rev. Lett.* **97,** 157403 (2006).
17. Shalaev, V. M. Optical negative-index metamaterials. *Nat. Photonics* **1,** 41–48 (2007).
18. Choi, M. *et al.* A terahertz metamaterial with unnaturally high refractive index. *Nature* **470,** 369–373 (2011).
19. Alů, A. & Engheta, N. The quest for magnetic plasmons at optical frequencies. *Opt. Express* **17,** 5723–5730 (2009).
20. Alů, A., Salandrino, A. & Engheta, N. Negative effective permeability and left-handed materials at optical frequencies. *Opt. Express* **14,** 1557–1567 (2006).
21. Vallecchi, A., Albani, M. & Capolino, F. Collective electric and magnetic plasmonic resonances in spherical nanoclusters. *Opt. Express* **19,** 2754–2772 (2011).
22. Mirin, N. A. & Halas, N. J. Light-bending nanoparticles. *Nano Lett.* **9,** 1255–1259 (2009).
23. Ginzburg, P., Berkovitch, N., Nevet, A., Shor, I. & Orenstein, M. Resonances On-Demand for Plasmonic Nano-Particles. *Nano Lett.* **11,** 2329–2333 (2011).
24. Plum, E. *et al.* Metamaterial with negative index due to chirality. *Phys. Rev. B* **79,** 035407 (2009).
25. Schurig, D. *et al.* Metamaterial Electromagnetic Cloak at Microwave Frequencies. *Science* **314,** 977–980 (2006).
26. Pendry, J. B., Schurig, D. & Smith, D. R. Controlling electromagnetic fields. *Science* **312,** 1780–1782 (2006).
27. Chen, H., Chan, C. T. & Sheng, P. Transformation optics and metamaterials. *Nat. Materials* **9,** 387–396 (2010).
28. Genov, D. A., Zhang, S. & Zhang, X. Mimicking celestial mechanics in metamaterials. *Nat. Physics* **5,** 687–692 (2009).
29. Li, J. & Pendry, J. B. Hiding under the carpet: a new strategy for cloaking. *Phys. Rev. Lett.* **101,** 203901 (2008).
30. Koo, S., Cho, C., Jeong, J.-H. & Park, N. Acoustic omni meta-atom for decoupled access to all octants of a wave parameter space. *Nat. Commun.* **7,** 13202 (2016).
31. Bückmann, T. *et al.* An elasto-mechanical unfeelability cloak made of pentamode metamaterials. *Nat. Commun.* **5,** 4130 (2014).
32. Oh, J. H., Kwon, Y. E., Lee, H. J. & Kim, Y. Y. Elastic metamaterials for independent realization of negativity in density and stiffness. *Sci. Rep*. **6,** 23630 (2016).
33. Hu, F.-G., Song, J. & Kamgaing, T. Modeling of multilayered media using effective medium theory. *EPEPS, IEEE 19th Conference on* 225–228 (2010).
34. Kang, J. H., Kim, D. S. & Park, Q.-H. Local capacitor model for plasmonic electric field enhancement. *Phys. Rev. Lett.* **102,** 093906 (2009).
35. Seo, M. A. *et al.* Terahertz field enhancement by a metallic nano slit operating beyond the skin-depth limit. *Nat. Photon*. **3,** 152–156 (2009).
36. Koo, S., Kumar, M. S., Shin, J., Kim, D. & Park, N. Extraordinary magnetic field enhancement with metallic nanowire: role of surface impedance in Babinet's principle for sub-skin-depth regime. *Phys. Rev. Lett.* **103,** 263901 (2009).
37. García-Vidal, F. J., Moreno, E., Porto, J. A. & Martín-Moreno, L. Transmission of light through a single rectangular hole. *Phys. Rev. Lett.* **95,** 103901 (2005).
38. Seo, M. A. *et al.* Active terahertz nanoantennas based on VO_2 phase transition. *Nano Lett.* **10,** 2064–2068 (2010).

Acknowledgements

This study was supported by the National Research Foundation funded by the Ministry of Science, ICT and Future Planning (Global Frontier Program: No. NRF-2014M3A6B3063708 and Global Research Laboratory: No. NRF-2008-00580).

Author Contributions

S.K. devised the structure of meta-atom and performed the theoretical deviation, and numerical analysis. N.P. conceived the idea for the top-down design of meta-atom structure, and encouraged S.K. to develop analytical model. D.M., N.P. and Y.K. checked the theoretical deviations, reviewed the manuscript, and wrote the manuscript with S.K.

Additional Information

Supplementary information accompanies this paper at http://www.nature.com/srep

Competing financial interests: The authors declare no competing financial interests.

How to cite this article: Koo, S. *et al.* Top-down, decoupled control of constitutive parameters in electromagnetic metamaterials with dielectric resonators of internal anisotropy. *Sci. Rep.* **7**, 42447; doi: 10.1038/srep42447 (2017).

Publisher's note: Springer Nature remains neutral with regard to jurisdictional claims in published maps and institutional affiliations.